International Journal of Emerging Technology and Advanced Engineering
Website: www.ijetae.com (ISSN 2250-2459, ISO 9001:2008 Certified Journal, Volume 3, Issue 7, July 2013)

Dye-Sensitized and Amorphous Silicon Photovoltaic (PV) Devices' Outdoor Performance: A Comparative Study

Otakwa, R.V.M.[1], Simiyu, J.[2], Mwabora, J.M.[3]

[1,2,3]*Department of physics, College of Biological and Physical Sciences, University of Nairobi, PO Box 30179 - 00100 GPO, Nairobi, Kenya*

[1]*Daystar University, Nairobi Campus, Department of Science, PO Box 44400 – 00100 GPO Nairobi, Kenya*

***Abstract*—The performance of a dye-sensitized solar module (DSSM) has been investigated under different air mass (*AM*), irradiance intensity and temperature conditions in Nairobi, Kenya. The good response of the DSSM to short wavelength radiation made it perform well at increased *AM* values as compared to what is reported of Amorphous Silicon (a-Si) photovoltaic (PV) devices. The DSSM performed better compared to what is reported of a-Si PV devices under irradiance and temperature dependence. The results are useful in PV sizing, especially in the area of Building Integrated Photovoltaics (BIPV) in Kenya and the tropics.**

***Keywords*— Dye-Sensitized, Amorphous Silicon, Outdoor Performance, Air Mass, Irradiance, Temperature**

I. Introduction

The need to switch to using renewable energy is on the rise world over. Fossil fuel reserves that have been depended on for energy supply are quickly diminishing, [1], leading to volatility in energy prices, [2]. The geopolitical issues experienced by countries with fossil fuel reserves further compound the grim situation. These factors have been key in denying many people access to energy, with those at the bottom of the economic pyramid being the most affected, [3]. The over-reliance upon fossil fuels by the world, [4] has also been associated with environmental effects, like global warming and its consequences, [5]. These have adversely affected life on earth, [6]. Adoption of energy sources that are alternative to fossil fuels is imperative. Renewable energy sources offer the most sustainable way forward, [7]. These include biomass, geothermal, tidal or wave power, water cycle or hydro, wind, and solar radiation.

The most abundant and fairly distributed of these is solar radiation – with about 3.9×10^{24} joules of solar energy reported to be reaching the earth annually, [8]. Apart from being abundant in supply, solar energy is used to produce heat for direct use or for further conversion to electricity through the thermal conversion pathway. It is also converted directly to electricity through the solar photovoltaic (PV) conversion pathway by exciting electrons in a solar cell.

The PV conversion pathway is the most espoused, [8], though the cost of PV systems is currently still high. However, efforts aimed at reducing solar PV prices, including enhancing efficiency and using cheaper fabrication materials have been on-going. Work on dye sensitized solar cells (DSSCs) has been part of these extensive efforts, [9].

Apart from using cheaper fabrication materials, DSSCs also promise cheaper electricity because they can be fabricated under less stringent conditions, [10]. Despite these accolades in respect of the DSSC technology, not much is being done to enhance its adoption in developing economies, but instead, Amorphous Silicon (a-Si), despite its performance challenges, is preferred by solar PV consumers in these countries to mono and poly crystalline silicon. In this work, the performance of a commercially available DSSC modules investigated under different air mass (*AM*), irradiance intensity and temperature values is reported and the results compared with what has been reported of a-Si PV devices operating under similar outdoor weather conditions.

II. Theory

Current density-Voltage (J-V) Characterization

A PV device's response is determined by its *J-V* characteristics. *J-V* characteristics are modeled according to the equation, [11],

$$J = J_L - J_s \exp\left[\frac{V + R_s J}{m V_T}\right] - \sigma V \quad (1)$$

Where J, J_L, J_s, V, m, V_T, R_s, J, and σ are the ideal current density, current density from the source, saturation current density, voltage across the PV terminals, the ideality factor, series resistance and shunt conductance respectively.

From equation 1, the photo-generated current density can be plotted as a function of the applied bias voltage. This results in a curve typically known as the current density-voltage (*J-V*) characteristic curve.

International Journal of Emerging Technology and Advanced Engineering
Website: www.ijetae.com (ISSN 2250-2459, ISO 9001:2008 Certified Journal, Volume 3, Issue 7, July 2013)

From the *J-V* curve, key parameters; V_{oc}, J_{sc}, J_s, *FF*, R_s, R_{sh} can be extracted and, *m* and η computed. V_{oc} is the voltage measured when the terminals of the PV device are isolated. This relates to the condition when the potential difference is at its maximum value. It is obtained from [11]:

$$V_{oc} = mV_T ln\frac{J_{ph}}{J_s} \qquad (2)$$

Where J_{ph}, J_s, V_{oc}, *m* and V_T are the photo-generated, saturation current densities, the open circuit voltage, the ideality factor and thermal voltage respectively.

FF is influenced by the series and shunt resistances. It measures the quality of a PV device. The squareness of a PV device's *J-V* curve indicates the quality of the device. It is calculated from:

$$FF = \frac{P_m}{V_{oc}J_{sc}} = \frac{J_{mp}V_{mp}}{V_{oc}J_{sc}} \qquad (3)$$

Where *FF*, P_m, V_{oc}, J_{sc}, J_{mp} *and* V_{mp} are the fill factor, maximum power, the open circuit voltage, the short circuit current density, the maximum power current density and the maximum power voltage respectively.

III. Experimental

A. Materials

One functional dye-sensitized solar module (DSSM) was used in this study. The module; Omny 11200 outdoor module - model number HS Code 85414090 was used as supplied by G24 Innovations Limited (UK). It was made up of 11 cells, rated 0.5 peak wattage and 8 peak voltage. The overall module thickness (including the encapsulation) was 0.59 cm. The active area of each cell was 15.92 cm^2; bringing the total active area of the module to 175.12 cm^2.

Other apparatus used in the study were a geometrical protractor and a metre rule supplied by Textbook Centre Limited (TBC), Kenya, a tilt-able metal rack supplied by Solargent Limited, Kenya, a 6 cm immersion thermometer (lower and upper limits – 0°C and 60°C), supplied by Griffin & George Limited, UK, a GTH 1160 NiCr-Ni digital thermocouple sensor supplied by TC limited, UK, a Raytek® *Plus* laser beam thermometer supplied by Raytek, USA, a CM3-pyranometer supplied by Kipp & Zonen, Delft/Holland, a Haenni solar 130 radiation meter supplied by Jenensfort, Switzerland, a DT9205A$^+$ digital multimeter supplied by Taurus Electronics Limited, Kenya, a Tektronix TDS 3032 digital phosphor oscilloscope supplied by Tektronix inc., USA, a Keithley 2400 digital source meter supplied by Keithley inc., USA, a Laboratory Virtual Engineering Workbench (LabVIEW^{TM}) application software supplied by National Instruments inc., USA, a desktop computer supplied by Hewlett-Packard (HP), Kenya and an IEEE-488 GPIB cable supplied by National Instruments inc., USA.

B. Methods

The study was carried out at the Department of Physics, University of Nairobi, Kenya. The DSSM was fixed on the tilt-able metal rack and the CM3-pyranometer positioned in the plane of array. The set-up was placed on the roof-top of the Department of Physics, University of Nairobi at a suitable place where shadows could not be cast on either the DSSM or the pyranometer. The DSSM was connected to the Keithley 2400 Source Meter using alligator clips. The Keithley source meter was connected to the HP desktop computer (with LabVIEW ^{TM} application software installed) via an IEEE-488 GPIB interface. To the pyranometer, the DT9205A$^+$ digital multimeter was connected to facilitate acquisition of irradiance data.

Current-voltage readings were first acquired at normal incidence to the incoming solar beam radiation by varying the tilt to coincide with the optimum tilt angle at the time. Optimum tilt angle was obtained from the air mass *versus* optimum tilt angle calibration curve. Both the ambient and module temperatures at the time of the *J-V* measurement acquisition were recorded. Ambient temperatures were measured using the 6 cm immersion thermometer – measurements that were corroborated with those from the Kenya Meteorological Department. Module temperatures were obtained by attaching the GTH 1160 NiCr-Ni digital thermocouple sensor to the back side of the module and recording the readings.

Readings from the thermocouple sensor were checked by simultaneously pointing a laser beam from the Raytek® *Plus* laser beam thermometer at about one meter perpendicular to the module and obtaining the temperature reading on top of the module. *J-V* measurements were obtained at different module temperatures and radiation intensities. The effects of air mass and hence, tilt angles were also investigated.

IV. Results And Discussion

Table 1 and figure 1 present the *J-V* characteristics of the DSSM obtained between *AM* 1 and *AM* 1.09.

International Journal of Emerging Technology and Advanced Engineering
Website: www.ijetae.com (ISSN 2250-2459, ISO 9001:2008 Certified Journal, Volume 3, Issue 7, July 2013)

Table 1:
Variation in the DSSM's *J-V* Characteristics at different times and *AM*.

AM	1	1.01	1.02	1.04	1.05	1.08	1.09
Time (Hrs)	1245	1300	1200	1100	1400	1000	1500
V_{oc} (V)	8.31	8.24	8.09	8.07	8.32	8.07	8.14
J_{sc} (Acm^{-2}) x 10^{-2}	1.04	1.01	9.84	9.66	7.84	7.69	5.68
FF	0.51	0.52	0.57	0.56	0.56	0.47	0.63
η (%)	1.77	1.75	1.88	2.26	1.27	1.06	1.19

As can be obtained from table 1 and figure 1, V_{oc} reduced linearly by 2.05% from 8.31 V at *AM* 1 to 8.14 V at *AM* 1.09. This can be attributed to the reduction in photo-generation at higher *AM* resulting mainly from attenuation of the effective component of the incident radiation that is necessary for PV effect. Studies have reported reduced irradiance intensities at higher *AM* [12], which explains the reduction in V_{oc} as observed in this work. The atmospheric attenuation is normally due to Rayleigh scattering, scattering by aerosols and atmospheric absorption through constituent gases (oxygen, ozone, water vapor and carbon dioxide). They cause the power of incident light (P_{in}) to reduce and also take longer optical path to the earth's surface, [13]. The density of electrons that get photo-ejected to conduct electricity, therefore reduce at higher *AM*, leading to lower V_{oc}. Studies on a-Si have reported a linear increase in V_{oc} of about 2.12% with increase *AM* [14].

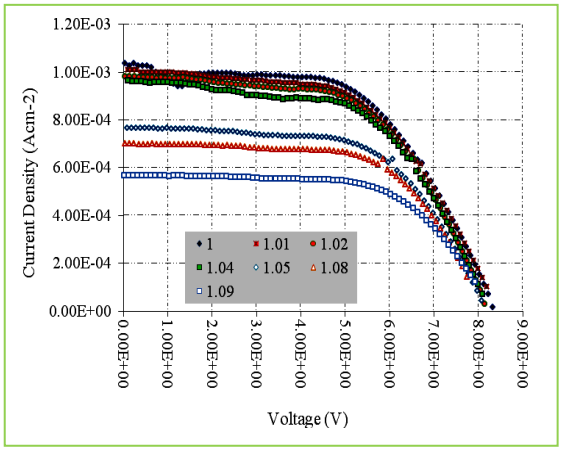

Figure 1: *J-V* characteristics for the DSSM at different values of air mass.

J_{sc} reduced by 26.06% from $1.04x10^{-3}$ Acm^{-2} to $7.69x10^{-4}$ Acm^{-2} as *AM* increased from 1 to 1.09. Reduction in J_{sc} as *AM* increased has also been reported in other DSSC studies, [15]. This reduction can be associated with decrease in the density of carriers as *AM* increases. An increase in V_{oc} leads to a logarithmic decrease in J_{ph}, and hence J_{sc}; a relationship that theoretically explains the J_{sc} trend. Studies on a-Si have also reported decrease in J_{sc} with increase in *AM* [16, 17]. A reduction in J_{sc} of 61.84% has been reported under conditions similar to those under which the DSSM was investigated, [14].

The DSSM's *FF* increased by 19.05% from 0.51 at *AM* 1 to 0.63 at *AM* 1.09. This indicates that the DSSM responded favorably to shorter wavelength radiation. Short wavelength radiation, ranging between 200 – 300 μm is prevalent at higher *AM*. The reduction in V_{oc} and J_{sc} led to this increase in *FF*. This indicates the DSSM's favorable response to shorter wavelength radiation, since short wavelength radiation. Studies conducted on a-Si under similar conditions have reported a reduction of 41.94% in *FF* with increase in *AM* [14], which shows a-Si's poor response to short wavelength radiation or diffuse light.

Closely associated with *FF*, V_{oc} and J_{sc} is efficiency, η. The η of the DSSM increased by 27.68% from 1.77% to 2.26% as *AM* increased from 1 to 1.04. It then reduced to 1.27%, 1.06% and 1.19% at *AM*1.05, *AM*1.08 and *AM*1.09 respectively. The behavior can be attributed to the good response of the DSSM to low wavelength radiation as well the increase in *FF*. Studies by Hinsch [18] have also reported similar behavior. On their part, a-Si PV modules are reported to have a narrow spectral response and do not perform well in the red rich part of the spectrum [19]. Studies on the behavior of η with increase in *AM* have reported declining η as *AM* increased [17], with a 29.17% reduction in η reported as *AM* increased under conditions similar to those under which the DSSM was investigated [14].

In figure 2, performance of the DSSM in the morning hours (0650 – 1200 hours) as compared to the afternoon hours (1201 to 1850 hours) is illustrated. Better performance was observed during the afternoon than morning hours. This can be attributed to presence of more atmospheric gaseous absorbers like H_2O, O_2, O_3 and CO_2 during the morning than afternoon hours [20].

International Journal of Emerging Technology and Advanced Engineering
Website: www.ijetae.com (ISSN 2250-2459, ISO 9001:2008 Certified Journal, Volume 3, Issue 7, July 2013)

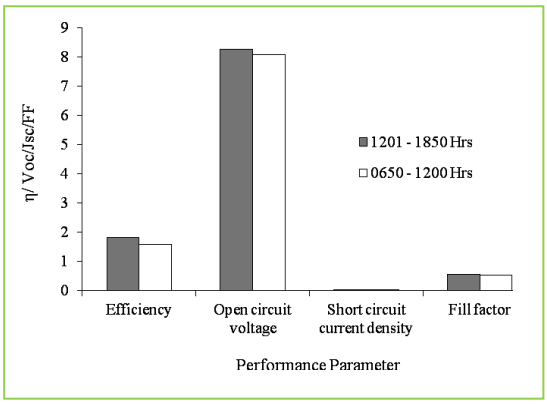

Figure 2: Comparative performance of the DSSM in the morning (0650 – 1200 hours) and in the afternoon (1201 – 1850 hours).

These absorbers lead to increased atmospheric turbidity and Rayleigh scattering in the morning than in the afternoon hours, resulting in the extinction of solar beams [21, 22], which affects *AM* values by varying the intensity of the direct component of sunlight [23]. a-Si PV modules have a stronger dependence on irradiance than the DSSM. They peak their performance closer to *AM* 1, when irradiance is highest, [17]. As *AM* influences both the intensity and spectral distribution of the solar beam reaching the earth's surface [24], an understanding of irradiance-dependence of the DSSM as compared to a-Si module as presented in the next section is vital.

Closely linked to the study on *AM* is the irradiance-dependence of the DSSM's *J-V* characteristics. Irradiance intensity holds great influence for solar cell performance, [25]. Table 3, figure 4 and figure 5 present the DSSM's *J-V* characteristics acquired between 653 Wm^{-2} and 1095.7 Wm^{-2} irradiance intensities. From figure 3, it can be observed that the voltage-controlled sections of the *J-V* characteristics shifted away from the origin and become steeper in slope as irradiance intensity increased; signifying reduction in R_s as irradiance intensity increased. This connotes reduction in the bulk resistance of the semiconductor used in the fabrication, which is good for the PV device.

The *J-V* characteristics show how J_{sc} significantly dependents on irradiance intensity. An analysis of how the characteristics varied with intensity is presented in table 3 and figure 5.

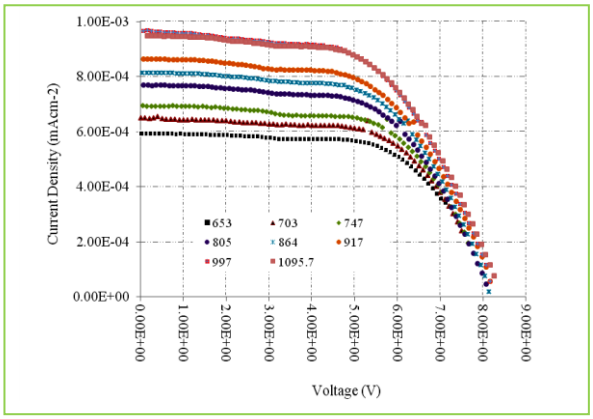

Figure 4: *J-V* characteristics of the DSSM at different irradiance intensities.

Table 3:
Variation of the DSSM's *J-V* characteristics at different irradiance intensities

Irradiance Intensity (Wm^2)	V_{oc} (V)	J_{sc} (Acm^{-2})	FF	η (%)
635	7.12	$5.92x10^{-4}$	0.73	3.39
703	7.50	$6.50x10^{-4}$	0.67	3.14
747	7.65	$6.93x10^{-4}$	0.66	3.07
805	8.07	$7.69x10^{-4}$	0.60	2.80
864	8.14	$8.14x10^{-4}$	0.60	2.73
917	8.17	$8.66x10^{-4}$	0.58	2.61
997	8.14	$9.66x10^{-4}$	0.57	2.60
1095.7	8.19	$9.48x10^{-4}$	0.58	2.42

International Journal of Emerging Technology and Advanced Engineering
Website: www.ijetae.com (ISSN 2250-2459, ISO 9001:2008 Certified Journal, Volume 3, Issue 7, July 2013)

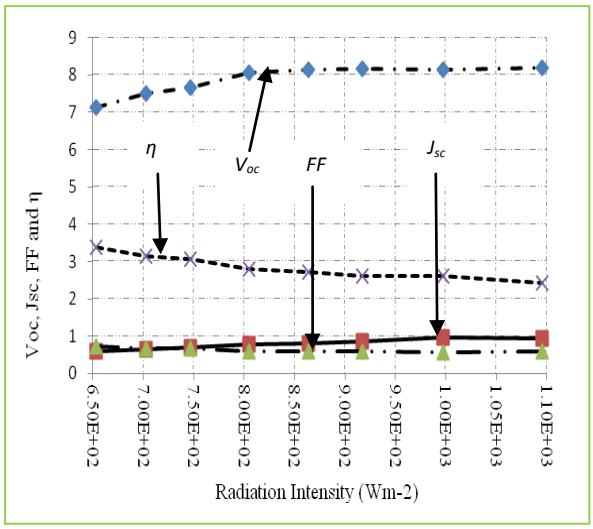

Figure 5: Illustration of how V_{oc}, J_{sc}, *FF* and η vary with irradiance.

V_{oc} for the DSSM increased linearly by 11.94% between 7.12 V and 8.07 V from 653 Wm^{-2} to 805 Wm^{-2}. Between 805 Wm^{-2} and 1095.7 Wm^{-2} irradiance intensities, increase in V_{oc} slowed by 1.49% to 8.19 V. This affirms the discussion under the DSSM's *AM* response, that the DSSM favored low irradiance intensities.

J_{sc} increased linearly by 64.41% between $5.92x10^{-4}$ Acm^{-2} and $9.66x10^{-4}$ Acm^{-2} from 653 Wm^{-2} to 997 Wm^{-2} irradiance intensities. From 997 Wm^{-2} to 1095.7 Wm^{-2} irradiance intensities, J_{sc} decreased linearly by 2.06% between $9.66x10^{-4}$ Acm^{-2} and $9.48x10^{-4}$ Acm^{-2}. The increase in J_{sc} between 653 Wm^{-2} and 997 Wm^{-2} can be attributed to increased photo-generation with increase in irradiance intensity. The good spectral response of the DSSM to short wavelength radiation helped in the rapid increase in J_{sc} under one sun as compared to during more than one sun.

The decrease in J_{sc} between 997 Wm^{-2} and 1095.7 Wm^{-2} irradiance intensities indicates a narrow response of the DSSM to short wavelength solar spectrum. This points to the DSSM's fabrication; intended use in weather conditions that do not experience more than one sun. *FF* of the DSSM showed a 20.55% linear improvement of between 0.58 and 0.73 as irradiance intensity reduced from 1095.7 Wm^{-2} to 653 Wm^{-2}. The increase in *FF* as irradiance intensity reduced can be linked to the reduction in charge leakages under low irradiance intensities, mainly due to low incidences of recombinations, and resistance in charge transfer. In a-Si PV modules, *FF* has been reported to increase by 125.70% between 300 Wm^{-2} and 600 Wm^{-2} irradiance intensities and to reduce by 23.69% between 600 Wm^{-2} to one sun [14].

The DSSM's η increased linearly by 5.74% from 4.70% to 4.97% as irradiance intensity increased from 653 Wm^{-2} to 747 Wm^{-2}, after which it reduced linearly by 8.65% to 4.54% as irradiance intensity increased from 747 Wm^{-2} to 1095.7 Wm^{-2}. The initial increase can be linked to the influence of increase in V_{oc}, J_{sc} and *FF* as irradiance intensity increased to 747 Wm^{-2}. Similar results have been reported by a number of studies, [25, 26]. The decrease observed after the 747 Wm^{-2} irradiance intensity can be linked to the decrease in V_{oc}, J_{sc} and *FF* at high radiation intensities.

Studies on a-Si modules have reported η to increase as irradiance intensity increases. This is because of the strong irradiance-dependence of V_{oc} and J_{sc}, [14, 26, 27]. a-Si has shown an increase in η observed between 300 Wm^{-2} and 600 Wm^{-2} irradiance intensities to be 80.95%, and a reduction of 26.72% observed between 600 Wm^{-2} irradiance intensity and one sun.

On the effect of the surface temperature, figure 6 presents the *J-V* characteristics for the DSSM obtained between 31.6˚C and 43.8˚C module surface temperatures.

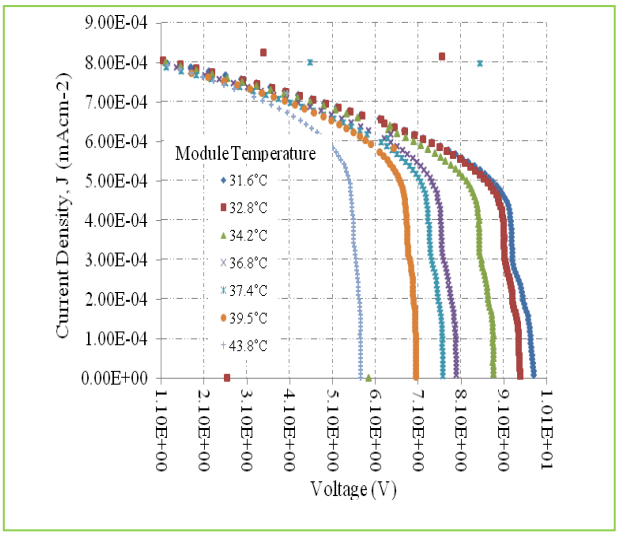

Figure 6: *J-V* characteristics of the DSSM at different module surface temperatures.

From the figure, V_{oc} is observed to be strongly influenced by temperature unlike J_{sc}. As the DSSM voltage increased from short circuit condition, the *J-V* characteristics became steeper at J_{sc} as temperature increased. Steeper slopes signify reduced R_{sh}. Table 4 and figure 7 present analyses on the module surface temperature effect on the DSSM's V_{oc}, J_{sc}, *FF* and η.

International Journal of Emerging Technology and Advanced Engineering
Website: www.ijetae.com (ISSN 2250-2459, ISO 9001:2008 Certified Journal, Volume 3, Issue 7, July 2013)

Table 4
Variation of the DSSM's *J-V* characteristics at different module surface temperatures.

Module Surface Temperature (˚C)	V_{oc} (V)	J_{sc} ($mAcm^{-2}$) x10^{-4}	*FF*	η (%)
31.6	9.80	7.98	0.57	5.94
32.8	9.48	8.26	0.57	5.95
34.2	8.86	8.00	0.60	5.67
36.8	8.86	7.87	0.54	5.02
37.4	7.68	8.00	0.60	4.91
39.5	7.05	7.72	0.65	4.71
43.8	5.76	7.92	0.65	3.95

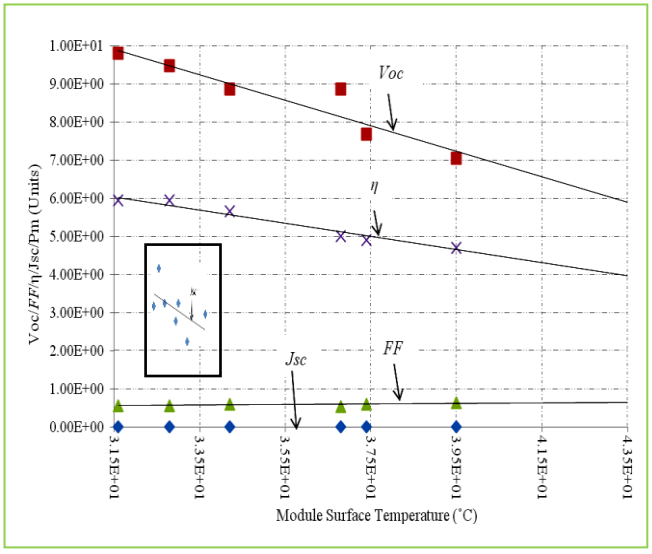

Figure 7: Relationship of *FF*, V_{oc}, η, J_{sc}, and P_m as functions of the DSSM surface temperature. [Inset is the relationship for J_{sc}, as a function of the DSSM surface temperature as the change was too small to be observed at the scale of the main figure].

V_{oc} decreases linearly by 41.22% from 9.80 V to 5.76 V as the DSSM surface temperature increased from 31.6˚C to 43.8˚C. A change of -0.33 V/˚C was observed. The decrease in V_{oc} with increase in temperature can be attributed to changes in charge carrier trapping and recombination centres that cause changes in charge distribution, coupled with the entropy that results from more electrons getting into excited states as temperature increases. This explains the temperature-dependence of V_{oc} as observed in equation 2.

An increase in resistivity to charge transport through the semiconductor nanoparticle network causes some of the electrons already injected into the CB of the semiconductor to migrate back to the HOMO level of the dye molecules or to the electrolyte due to electron trapping effects.

The decrease could also be as a result of radiative external quantum efficiency (REQE), [28]. Studies on a-Si have reported a decrease in V_{oc} as the module surface temperature increased [14]. Studies by Katherine [16] on amorphous silicon PV modules showed a linear decrease of 4% from 0°C to 5°C and 3% from 45°C to 80°C, at the rate of $8.89x10^{-2}$%°C^{-1} and $-8.86x10^{-2}$%°C^{-1} respectively. The DSSM's η was better than what has been reported of a-Si PV devices under temperature influence.

V. Conclusion

In this work, detailed experimental results showing how the Omny 11200 outdoor solar module's characteristics; V_{oc}, J_{sc}, *FF* and η were affected by *AM*; irradiance as well as module temperatures have been presented. The DSSM's V_{oc}, J_{sc}, *FF* and η improved as *AM* increased. This shows that the DSSM performs well under diffuse radiation. This is not true for a-Si solar modules. This finding is very helpful to solar electricity practitioners during PV sizing. If *AM* at a particular location is usually high, choosing DSSMs over a-Si would guarantee better results for the client. The DSSM's good performance under diffuse radiation shows the DSSM does not have to follow the north-south orientation rule. This means that DSSMs can be used as windows or walls in buildings irrespective of their orientations.

The orientation-dependence of a-Si modules does not allow for this flexibility hence limiting innovation in the design of Net Zero Energy buildings. The improved performance of the DSSM between 1201 hours and 1850 hours as compared to 0650 hours to 2010 hours when a-Si modules perform well shows that the two technologies (DSSM and a-Si) can be jointly used in the design of Net Zero Energy buildings. Better results for the DSSM at lower as compared to higher irradiance intensities makes it ideal for use in electronic consumer goods like laptops, calculators, etc, which by nature, are mainly used indoors. The attribute also makes the DSSM useful in complimenting a-Si solar modules, especially in Building Integrated Photovoltaics (BIPV) in areas known to have fluctuations in irradiance intensity.

The DSSM showed an overall benefit from a combination of high irradiance and elevated temperatures. a-Si modules are also reported to perform well at high irradiance levels and at high temperatures.

The design and development of buildings in areas with a combination of high irradiance and elevated temperatures would benefit from both the DSSC technology and a-Si solar cell technology. During PV sizing for buildings in such areas however, the DSSC technology would be the BIPV of choice.

Acknowledgments

The support given by African PRIDE Centre (APC) and Sustainable Energies and Solutions Limited (SEAS) during the period that this work was undertaken is acknowledged and greatly appreciated.

REFERENCES

[1] Murray, J. and King, D., (2012). Climate Policy: Oil's Tipping Point has Passed. Nature 481, 433 – 435.

[2] Timmer, J., (2012). We've Hit 'Peak Oil'; Now Comes Permanent Price Volatility. Arstechnica.com [accessed on 14 March 2012 at http://arstechnica.com/science/news/2012/01].

[3] Barnes, D. and Toman, M., (2006). Energy, Equity and Economic Development. In economic development and environmental sustainability. Oxford University Press, 1 – 52.

[4] Heymann, E. (2011). Carbon Capture and Storage for Climate Protection – Important, Tedious and Costly. Deutsche Bank, 1 – 5.

[5] Dincar, I., (2003). The Role of Energy in Energy Policy Making. Energy Policy, 30, 137 – 149.

[6] Muoghalu, J. (2003). Priority Parameters: Abiotic and Biotic Components. In environmental monitoring edited by Inyang, H. and Daniels, J.). Encyclopaedia of Life Support Systems (EOLSS), 1 – 8.

[7] Bárd, H. (2012). Buy Coal! A case for Supply-Side Environmental Policy. Journal of Political Economy, 120 (1): 77 DOI: 10.1086/665405.

[8] Rabah, K., Ndjeli, L. and Raturi, A., (1995). Review of PV Energy Development in Kenya for Rural Electrification. International Centre for Theoretical Physics (ICTP), 95, 4817.

[9] Nwanya, A., Ezema, F. and Ejikeme, P., (2011). Dye Sensitized Solar Cells: A Technically and Economically Alternative Concept to p-n Junction Photovoltaic Devices. International Journal of Physical Sciences, 6, (22), 5190 – 5201.

[10] O'Regan, B. and Grätzel, M., (1991). A Low Cost, High Efficiency Solar Cell based on Dye-Sensitized Colloidal TiO_2 Films. Nature, 353, 737 - 739.

[11] Otakwa, R.V.M, Simiyu, J., Waita, S.M., Mwabora, J.M., (2012), Application of Dye-Sensitized Solar Cell Technology in the Tropics: Effects of Air Mass on Device Performance, International Journal of Renewable Energy Research, 2 (3), 369 – 375.

[12] Meinel, A. and Meinel, M., (1976). Applied Solar Energy. Addison Wesley Publishing Company, 10 – 78.

[13] Antŏn, M., Serrano, A., Cancillo, M. and Garcia, J., (2009). Influence of the Relative Optical Air Mass on Ultraviolet Erythermal Irradiance. Journal of Atmospheric and Solar Terrestrial Physics, 71 (17-18), 2027 – 2030.

[14] Ugwoke, P., (2012). Performance Assessment of Three Different Photovoltaic Modules as a Function of Solar Insolation in South Eastern Nigeria, International Journal of Applied Science and Technology, 2 (3), 319 – 327.

[15] Katrine, F., (2008). Performance Comparison of a DSSC and a Silicon Solar Cell under Idealized and Outdoor Conditions. M.Sc. Thesis for the Technical University of Denmark, 106 – 110.

[16] Katherine, L., (2010), Photovoltaic Cell Efficiency at Elevated Temperatures, B.Sc. Thesis for the Department of Mechanical Engineering, Massechusetts Institute of Technology, 1 – 23.

[17] Chagaar, M. and Mialhe, P., (2008). Effects of Atmospheric Parameters on the Silicon Solar Cells Performance, Journal of Electron Devices, 6, 173 – 176.

[18] Hinsch, A., (2007). DSSCs for Façade Applications: Recent Results from Project Colorsol, 17th International Photovoltaic Science Engineering Conference, 3 – 7 December, 2007, Fukuoka, Japan.

[19] Chianese, D., Skoezek, A., Virtuari, A. and Ceberauer, T., (2011). Energy Yield Prediction of a-Si Photovoltaic Modules using Full Data Series of Irradiance and Temperature for Different Geographical Locations, 26th European Photovoltaics Solar Energy Conference, September, 2011, Hamburg, Germany, 1- 7.

[20] Louche, A., Maurel, M., Simonnot, G., Peri, G. and Igbal, M., (2000). Determination of Angstrom's Turbidity Coefficient from Direct Total Solar Irradiance Measurements, Laboratoire d'Helioenergetique, 1622 – 1630.

[21] Kasten, F. and Young, A., (1989). Revised Optical Air Mass Tales and Approximation Formula, Applied Optics, 28 (22), 4735 – 4738.

[22] Hahn, D., (2009). Light Scattering Theory, In Lecture Notes, Department of Mechanical and Aerospace Engineering, University of Florida, 1 – 13.

[23] Thavasi, V., Renugopalakrishnan, V., Jose, R. and Ramakrishna, S., (2009). Controlled Electron Injection and Transport in Material Interfaces in DSSCs, Materials Science and Engineering: Reports, 63, 81 – 99.

[24] Nayaab, M., Karayel, M., Neeman, E. and Selkowitz, S., (1983). Analysis of Atmospheric Turbidity for Daylight Calcultations, International Daylight Conference, Phoenix AZ, February, 16 – 18, 1 – 23.

[25] Dinçer, F. and Meral, M., (2010). Critical factors affecting efficiency of solar cells. Smart Grid and Renewable Energy, 1, 47 – 50.

[26] Jensen, K., (2008). Performance comparison of a DSSC and a silicon solar cell under idealized and outdoor conditions. M.Sc. Thesis for the Technical University of Denmark, 1 – 131.

[27] Ghoneim, A., Kandil, K., Al-Hasan, A., Altouq, M., Al-asaad, A., Alshamari, L. and Shamsaldein, A., (2011). Analysis of performance parameters of amorphous silicon modules under different environmental conditions. Energy Science and Technology, 2 (1), 43 – 50.

[28] Martin, A., (2003). General Temperature Dependence of Solar Cell Performance and General Implications for Device Modeling, Progress in Photovoltaics: Research and Applications, 11, 333 – 340.